Phys. Status Solidi B **248**, No. 11, 2688–2691 (2011) / **DOI** 10.1002/pssb.201100191

physica status solidi b
www.pss-b.com
basic solid state physics

Density of states deduced from ESR measurements on low-dimensional nanostructures; benchmarks to identify the ESR signals of graphene and SWCNTs

Péter Szirmai[1], Gábor Fábián[1], Balázs Dóra[1], János Koltai[2], Viktor Zólyomi[3,4], Jenő Kürti[2], Norbert M. Nemes[5], László Forró[6], and Ferenc Simon[*,1]

[1] Budapest University of Technology and Economics, Institute of Physics and Condensed Matter Research Group of the Hungarian Academy of Sciences, 1521 Budapest, Hungary
[2] Department of Biological Physics, Eötvös University, Pázmány Péter sétány 1/A, 1117 Budapest, Hungary
[3] Research Institute for Solid State Physics and Optics, Hungarian Academy of Sciences, P.O. Box 49, 1525 Budapest, Hungary
[4] Department of Physics, Lancaster University, Lancaster, LA1 4YB, United Kingdom
[5] GFMC, Departamento de Física Aplicada III, Univesidad Complutense, 28040 Madrid, Spain
[6] Laboratory of Physics of Complex Matter, FBS Swiss Federal Institute of Technology (EPFL), 1015 Lausanne, Switzerland

Received 27 May 2011, revised 30 August 2011, accepted 13 September 2011
Published online 7 October 2011

Keywords carbon nanotubes, electron spin resonance, graphene, Pauli susceptibility, spin-decoherence, spintronics, spin life-time

* Corresponding author: e-mail ferenc.simon@univie.ac.at, Phone: +36-1-4633816, Fax: +36-1-4634180

Electron spin resonance (ESR) spectroscopy is an important tool to characterize the ground state of conduction electrons and to measure their spin-relaxation times. Observing ESR of the itinerant electrons is thus of great importance in graphene and in single-wall carbon nanotubes. Often, the identification of CESR signal is based on two facts: the apparent asymmetry of the ESR signal (known as a Dysonian lineshape) and on the temperature independence of the ESR signal intensity. We argue that these are insufficient as benchmarks and instead the ESR signal intensity (when calibrated against an intensity reference) yields an accurate characterization. We detail the method to obtain the density of states from an ESR signal, which can be compared with theoretical estimates. We demonstrate the success of the method for K doped graphite powder. We give a benchmark for the observation of ESR in graphene.

1 Introduction Electron spin resonance (ESR) has proven to be an important method in identifying the ground state of strongly correlated electron systems. ESR helped e.g. to identify the ordered spin-density wave ground state in the Bechgaard salts [1] and for carbonaceous materials, ESR was key to synthesize the phase pure AC_{60} (A = K, Rb, Cs) fulleride polymer [2].

A natural expectation is that ESR can be applied for single-wall carbon nanotubes (SWCNTs) [3] and graphene [4], which are the two novel members of the carbon nanostructure family. The ESR literature on graphene is yet restricted to a single report [5]. Although there exists larger literature on the SWCNTs, the situation is yet unclear. In general, the ESR signal on itinerant electrons yields a direct measurement of the spin-relaxation time (often called as spin-decoherence time), T_1, through the relation: $T_1 = 1/\gamma \Delta B$, where ΔB is the homogeneous ESR linewidth and $\gamma/2\pi = 28.0\,\mathrm{GHz}/T$ is the electron gyromagnetic ratio. T_1 is the central parameter which characterizes the usability of the materials for spintronics. This explains the motivation of the ESR studies on graphene and SWCNTs.

One important question is whether the ESR signal of the itinerant (i.e. the conduction electrons) can be observed at all. It was argued on a theoretical basis [6] that it cannot be observed due to the Tomonaga-Luttinger liquid ground state of the metallic SWCNTs [7–9]. It seemed that the only way to explore the local magnetism in SWCNTs is to spin label it either by means of ^{13}C nuclei [10] or by an electron spin label [11]. The literature situation on the SWCNT ESR studies is conflicting, and it is reviewed herein without any judgement

on validity. Petit et al. [12] reported the observation of the ESR signal of itinerant electrons. Salvetat et al. [13] reported that the ESR signal occuring around $g \approx 2$ is caused by defects in the SWCNTs. Likodimos et al. [14] reported that a similar signal is related to the itinerant electrons with a possible antiferromagnetic order at low temperature. Corzilius et al. [15] reported the observation of the itinerant electron ESR in SWCNT samples prepared by chemical vapour deposition.

Often, the identification of the itinerant electron ESR signal is based on two facts: the asymmetry of the ESR lineshape (also known as a Dysonian) and the temperature independence of the ESR signal intensity. The Dysonian lineshape also occurs for localized spins (e.g. for paramagnetic impurities) which are embedded in a metal thus this property cannot be used for the above identification. This is discussed as Eqs. 3.7–3.8 in the seminal paper of Feher and Kip as the 'slowly diffusing magnetic dipole case' [16]. The temperature independence of the ESR intensity could be observed for localized paramagnetic spins when they are embedded in a metal with increasing conductivity, σ with decreasing temperature; then the microwave penetration depth $\lambda = \sqrt{2/(\mu_0 \omega \sigma)}$ (here μ_0 is the permeability of the vacuum and ω is the frequency of the microwaves).

There has been remarkable progress in the quest for the intrinsic ESR signal in SWCNTs using samples made of nanotubes separated according to their metallicity [17]. However, both kinds of samples, i.e. those made of purely metallic or semiconducting nanotubes show similar ESR signals [18], thus the situation remains unresolved.

A parallel situation happened for high T_c superconductors: soon after their discovery [19] several reports claimed to have observed the 'intrinsic' ESR signal in these compounds. Later it turned out for all studies that the signal of parasitic phases (which happen to have strong paramagnetic signals), the so-called green and brown-phases were observed. Later, spin labeling (e.g. Gd substituting Y in $YBa_2Cu_3O_{7-\delta}$) turned out to be successful to study the electronic structure [20].

The ESR signal of itinerant electrons in the SWCNTs is expected to have (i) a g-factor near 2, (ii) a line-width, ΔB smaller than 1 mT, and (iii) a signal intensity corresponding to the low density of states (DOS) with no temperature dependence. All properties present a significant hindrance for the signal identification since most impurity in carbon have $g \approx 2$, a maximum 1 mT line-width, and the Curie spin-susceptibility of even a small amount of impurity overwhelms the small Pauli susceptibility of the itinerant electrons. Since nothing is known about the g-factor and the line-width *a priori*, only the magnitude of the calibrated ESR signal when compared to the theoretical estimates of the Pauli spin-susceptibility provides a clear-cut ESR signal identification in graphene or SWCNTs.

Here, we outline the method to determine the calibrated ESR signal intensity and the resulting DOS in one- and two-dimensional carbon. The method is demonstrated for K doped graphite powder which is regarded as a model system of biased graphene [21]. A good agreement is obtained between the theoretical and experimental DOS for the KC_8 doped graphite system. We note, that a similar program was applied successfully when the ESR signals of Rb_3C_{60} [22] and MgB_2 [23] were discovered. We give benchmarks which can be used to decide whether the ESR of the itinerant electrons is observed in graphene.

2 Experimental We used commercial graphite powder (Fischer Scientific) and potassium (99.95% purity: Sigma–Aldrich) for the intercalation experiments. The graphite powder (3 mg) was mixed with 3 mg MnO:MgO powder (Mn concentration 1.5 ppm) and ground in a mortar. MgO separates the graphite powder pieces, which enables the penetration of exciting microwave and its Mn content acts as an ESR intensity standard. The mixture was vacuum annealed at 500 °C for 1 h in an ESR quartz tube and inserted into an Ar glove-box without air exposure. Alkali doping was performed by heating the ESR quartz tube containing the graphite powder and potassium for 29 h using the standard temperature gradient method in Ref. [24] to obtain Stage I, i.e. KC_8 intercalated graphite. ESR measurements were performed with a JEOL X-band spectrometer at room temperature. Derivative Lorentzian curves were fitted to obtain the signal intensities. Error of the fit is about 1%, however the ESR intensity measurement is proun to systematic errors such as the spectrometer tuning, sample placement etc. which gives rise to an error of 5–10%.

3 Results and discussion First, we discuss spin-susceptibility, χ_s, calculated from the ESR signal in different dimensions. ESR spectroscopy measures the net amount of magnetic moments, which is an extensive thermodynamic variable, i.e. proportional to the sample amount. The corresponding intensive variable, which characterizes the material is the spin-susceptibility, χ_s which reads as:

$$\chi_s = \mu_0 \cdot \frac{\sum m}{B_{res} \cdot V_D} \quad \text{(SI)}$$
$$\chi_s = \frac{\sum m}{B_{res} \cdot V_D} \quad \text{(Gaussian)} \qquad (1)$$

where m is the magnetic moment, B_{res} is the magnetic field of the resonance, V_D is the volume in D dimension ($D = 2;\ 3$), and μ_0 is the permeability of the vacuum. Clearly, the unit of χ_s depends on the dimension D.

χ_s is either due to the Curie spin-susceptibility for non-interacting spins or the Pauli spin-susceptibility for itinerant electrons in a metal. The relevant expressions are given in Table 1. Therein, A_c/V_c denotes the unit area/volume, g is the g-factor, μ_B is the Bohr moment and k_B is the Boltzmann constant. S is the spin state of the non-interacting spins and $\varrho(\varepsilon_F)$ is the DOS at the Fermi level in units of states/eV $\cdot$ *unit*. Here, *unit* refers to the unit chosen, e.g. for C_{60} fulleride salts, the unit could be 60 carbon atoms. Then the DOS is larger but so is the unit volume which

Table 1 The Curie and the Pauli spin-susceptibilities in three and two dimensions. Note that in two dimensions A_c replaces V_c in the expressions.

Curie susceptibility		Pauli susceptibility		units	
SI	Gaussian	SI	Gaussian	SI 3D (2D)	Gaussian 3D (2D)
$\mu_0 \frac{g^2 S(S+1)\mu_B^2}{3k_B T} \frac{1}{V_c}$	$\frac{g^2 S(S+1)\mu_B^2}{3k_B T} \frac{1}{V_c}$	$\mu_0 \frac{g^2\mu_B^2}{4} \varrho(\varepsilon_F) \frac{1}{V_c}$	$\frac{g^2\mu_B^2}{4} \varrho(\varepsilon_F) \frac{1}{V_c}$	1 (m)	$\frac{\text{emu}}{\text{cm}^3 \cdot \text{Oe}} \left(\frac{\text{emu}}{\text{cm}^2 \cdot \text{Oe}}\right)$

cancels in the result. For graphene, the two atom basis is used as *unit*.

The ESR intensity of a metal can be calibrated against a Curie spin system with known amount of spins. This leads to the comparison of the Pauli and the Curie spin-susceptibilities:

$$\frac{I_{ESR}(\text{Pauli})}{I_{ESR}(\text{Curie})} = \frac{\sum m_{\text{Pauli}}}{\sum m_{\text{Curie}}} = \left(\frac{g_{\text{Pauli}}}{g_{\text{Curie}}}\right)^2 \times \frac{4}{3} S(S+1) \times k_B T \varrho(\varepsilon_F) \frac{B_{res}(\text{Pauli})}{B_{res}(\text{Curie})} \frac{\left(\frac{V_D}{V_c(D)}\right)(\text{Pauli})}{\left(\frac{V_D}{V_c(D)}\right)(\text{Curie})} \quad (2)$$

where I_{ESR} denotes the ESR signal. V_D and $V_c(D)$ are the volume of the sample and the unit cell in D dimensions, respectively. Note that $V_D/V_c(D)(\text{Pauli}) = N(\text{Pauli})$ is the number of units in the metallic sample and $V_D/V_c(D)(\text{Curie}) = N(\text{Curie})$ is the number of Curie spins. Eq. (2) is correct for both SI and Gaussian units and is independent of the choice of *unit*, as expected.

For $S = 1/2$ and $g_{\text{Pauli}}, g_{\text{Curie}} \approx 2$, Eq. (2) simplifies to:

$$\frac{I_{ESR}(\text{Pauli})}{I_{ESR}(\text{Curie})} = k_B T \varrho(\varepsilon_F) \frac{N(\text{Pauli})}{N(\text{Curie})}. \quad (3)$$

We present the case of KC_8 as an example of the ESR intensity calibration. In Fig. 1, we show the ESR signal of the mixture of MnO:MgO and saturated K doped graphite. Parameters of the calibration are given in Table 2: C_{spin} is the

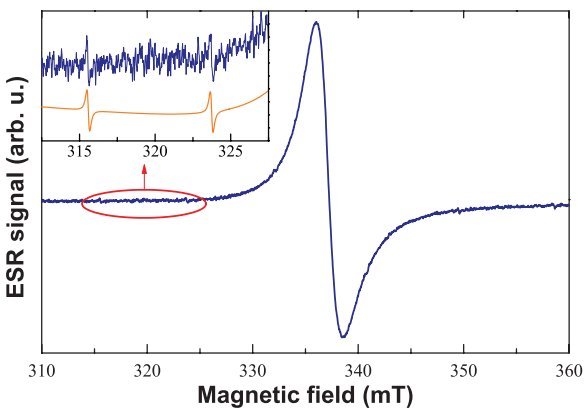

Figure 1 (online colour at: www.pss-b.com) ESR spectrum of saturated K doped graphite powder sample at $T = 300$ K. The inset is a zoom on the ESR spectrum and shows the two lowest lying lines of the Mn^{2+} hyperfine sextuplet. The solid curve is a fit.

spin concentration and the effective $\langle S \cdot (S+1) \rangle_{Mn^{2+}} = 9/4$ as only the $-1/2 \rightarrow 1/2$ transition is observed from the 5 Zeeman transitions of the Mn^{2+} ($S = 5/2$) [25].

The sample content gives: $N(\text{Pauli})/N(\text{Curie}) \approx 3.33$ and Eq. (2) yields $\varrho(\varepsilon_F) \approx 0.34(2)$ states/(eV · C atom), in good agreement with $\varrho(\varepsilon_F) = 0.327$ states/(eV · C atom) obtained by specific heat measurements [24].

In the following, we analyse the case of graphene. There, $A_c = 5.24$ Å^2/(unit cell) is the graphene elementary cell and the DOS, at $T = 0$ and $\Gamma = 0$ (Γ is the damping parameter), reads as a function of the chemical potential μ [26]:

$$\varrho(\mu) = \frac{2A_c \mu}{\pi \hbar^2 v_F^2}. \quad (4)$$

Here, $v_F \approx 10^6$ m/s is the Fermi velocity. Consequently, $\varrho(\mu) = \mu \cdot 0.0770$ states/(eV^2 · unit cell) if μ is measured in eV. Thus Eq. (3) (in two dimensions) at room temperature reads:

$$\frac{\sum m_{gr}}{\sum m_{\text{Curie}}} = \underbrace{0.026 \cdot 0.0770}_{\approx 1/500} \cdot \mu[\text{eV}] \frac{N(\text{gr})}{N(\text{Curie})}. \quad (5)$$

N(gr) is the number of graphene unit cells in the sample.

Finally, we assess the feasibility of ESR spectroscopy on graphene. ESR spectrometer performance is given by the limit-of-detection (LOD_0) i.e. the number of $S = 1/2$ Curie magnetic moments at room temperature which are required for a signal-to-noise ratio of S/N = 10 for $\Delta B = 0.1$ mT linewidth, and 1 s/spectrum-point time constant. For modern spectrometers $LOD_0 = 10^{10}$ spins/0.1 mT. To calculate the LOD for a broadened ESR line, LOD(ΔB), we introduce a function to track the effect of broadening:

$$f(\Delta B) = \begin{cases} \frac{\Delta B}{0.1\text{ mT}} & \text{if} \quad \Delta B \leq 1\text{ mT} \\ \frac{\Delta B^2}{0.1\text{ mT}^2} & \text{if} \quad \Delta B > 1\text{ mT}. \end{cases} \quad (6)$$

Table 2 Parameters of the χ_s calibration of KC_8.

	Mn:MgO	graphite
$\langle S \cdot (S+1) \rangle$	9/4	
M_{mol} [g/mol]	40	12
m [mg]	3	3
C_{spin}	1.5 ppm	1
I_{ESR}	$6 \cdot 5.3 \cdot 10^{-3}$	205

This function is 1 if $\Delta B = 0.1\,\mathrm{mT}$ and it is 10 if $\Delta B = 1\,\mathrm{mT}$ which is the usual maximum modulation amplitude. For line-widths above this value, the function grows quadratically, which describes that the amplitude of the derivative ESR signal drops quadratically. Using this function: $\mathrm{LOD}(\Delta B) = \mathrm{LOD}_0 \cdot f(\Delta B)$. Comparison with Eq. (5) yields that numerically (μ in eV units)

$$\mathrm{LOD}(\mathrm{gr}) = 500/\mu \cdot \mathrm{LOD}_0 \cdot f(\Delta B) \tag{7}$$

is the LOD for graphene. We could conclude that

$$A_{\mathrm{lb}}(\mathrm{gr}) = 500/\mu \cdot \mathrm{LOD}_0 \cdot f(\Delta B) \cdot A_{\mathrm{c}} \tag{8}$$

which gives a lower bound for the area of the graphene sheet which enables the ESR measurement. Assuming a $\Delta B = 0.1\,\mathrm{mT}$ and a shift in chemical potential by gate bias of $\sim$0.2 eV, we estimate $A_{\mathrm{lb}}(\mathrm{gr}) \approx 1.3\ \mathrm{mm}^2$.

4 Summary In summary, we detailed the method of obtaining the calibrated ESR intensity and the DOS in carbonaceous materials. We argue that a similar analysis is required for the identification of the ESR signal of itinerant electrons in SWCNT and graphene.

Acknowledgements This work was supported by the OTKA Grant Nr. K 81492, and Nr. K72613, by the ERC Grant Nr. ERC-259374-Sylo, the Marie Curie ERG project CARBOTRON, and by the New Széchenyi Plan Nr. TÁMOP-4.2.1/B-09/1/KMR-2010-0002. BD acknowledges the Bolyai programme of the Hungarian Academy of Sciences. The Swiss NSF and its NCCR "MaNEP" are acknowledged for support.

References

[1] J. B. Torrance, H. Pedersen, and K. Bechgaard, Phys. Rev. Lett. **49**, 881–884 (1982).
[2] O. Chauvet, G. Oszlányi, L. Forró, P. Stephens, M. Tegze, G. Faigel, and A. Jánossy, Phys. Rev. Lett. **72**(17), 2721–2724 (1994).
[3] S. Iijima and T. Ichihashi, Nature **363**, 603–605 (1993).
[4] K. S. Novoselov, A. K. Geim, S. V. Morozov, D. Jiang, Y. Zhang, S. V. Dubonos, I. V. Grigorieva, and A. A. Firsov, Science **306**, 666–669 (2004).
[5] L. Ćirić, A. Sienkiewicz, B. Náfrádi, M. Mionić, A. Magrez, and L. Forró, Phys. Status Solidi B **246**, 2558–2561 (2009).
[6] B. Dóra, M. Gulácsi, J. Koltai, V. Zólyomi, J. Kürti, and F. Simon, Phys. Rev. Lett. **101**, 106408 (2008).
[7] M. Bockrath, D. H. Cobden, J. Lu, A. G. Rinzler, R. E. Smalley, L. Balents, and P. L. McEuen, Nature **397**, 598–601 (1999).
[8] H. Ishii, H. Kataura, H. Shiozawa, H. Yoshioka, H. Otsubo, Y. Takayama, T. Miyahara, S. Suzuki, Y. Achiba, M. Nakatake, T. Narimura, M. Higashiguchi, K. Shimada, H. Namatame, and M. Taniguchi, Nature **426**, 540–544 (2003).
[9] H. Rauf, T. Pichler, M. Knupfer, J. Fink, and H. Kataura, Phys. Rev. Lett. **93**, 096805 (2004).
[10] P. M. Singer, P. Wzietek, H. Alloul, F. Simon, and H. Kuzmany, Phys. Rev. Lett. **95**, 236403 (2005).
[11] F. Simon, H. Kuzmany, B. Náfrádi, T. Fehér, L. Forró, F. Fülöp, A. Jánossy, L. Korecz, A. Rockenbauer, F. Hauke, and A. Hirsch, Phys. Rev. Lett. **97**, 136801 (2006).
[12] P. Petit, E. Jouguelet, J. E. Fischer, A. G. Rinzler, and R. E. Smalley, Phys. Rev. B **56**, 9275–9278 (1997).
[13] J. P. Salvetat, T. Fehér, C. L'Huillier, F. Beuneu, and L. Forró, Phys. Rev. B **72**, 075440 (2005).
[14] V. Likodimos, S. Glenis, N. Guskos, and C. L. Lin, Phys. Rev. B **76**, 075420 (2007).
[15] B. Corzilius, K. P. Dinse, K. Hata, M. Haluška, V. Skákalová, and S. Roth, Phys. Status Solidi B **245**, 2251–2254 (2008).
[16] G. Feher and A. F. Kip, Phys. Rev. **98**, 337–348 (1955).
[17] M. S. Arnold, A. A. Green, J. F. Hulvat, S. I. Stupp, and M. C. Hersam, Nature Nanotechnol. **1**(1), 60–65 (2006).
[18] M. Havlicek, W. Jantsch, M. Ruemmeli, R. Schoenfelder, K. Yanagi, Y. Miyata, H. Kataura, F. Simon, H. Peterlik, and H. Kuzmany, Phys. Status Solidi B **247**(11–12), 2851–2854 (2010).
[19] J. G. Bednorz and K. A. Müller, Z. Phys. B **64**, 189–193 (1986).
[20] A. Jánossy, J. R. Cooper, L. C. Brunel, and A. Carrington, Phys. Rev. B **50**(5), 3442–3445 (1994).
[21] A. Grueneis, C. Attaccalite, A. Rubio, D. V. Vyalikh, S. L. Molodtsov, J. Fink, R. Follath, W. Eberhardt, B. Buechner, and T. Pichler, Phys. Rev. B **79**(20), 205106 (2009).
[22] A. Jánossy, O. Chauvet, S. Pekker, J. R. Cooper, and L. Forró, Phys. Rev. Lett. **71**(7), 1091–1094 (1993).
[23] F. Simon, A. Jánossy, T. Fehér, F. Murányi, S. Garaj, L. Forró, C. Petrovic, S. L. Bud'ko, G. Lapertot, V. G. Kogan, and P. C. Canfield, Phys. Rev. Lett. **87**(4), (2001).
[24] M. S. Dresselhaus and G. Dresselhaus, Adv. Phys. **30**(2), 132 (1981).
[25] A. Abragam and B. Bleaney, Electron Paramagnetic Resonance of Transition Ions (Oxford University Press, Oxford, England, 1970).
[26] A. H. Castro Neto, F. Guinea, N. M. R. Peres, K. S. Novoselov, and A. K. Geim, Rev. Mod. Phys. **81**(1), 109–162 (2009).